doi:10.1111/evo.14205

Demographic consequences of dispersal-related trait shift in two recently diverged taxa of montane grasshoppers*

Joaquín Ortego,[1,2] Jorge Gutiérrez-Rodríguez,[1] and Víctor Noguerales[3]

[1]Department of Integrative Ecology, Estación Biológica de Doñana (EBD-CSIC), Seville, Spain

[2]E-mail: joaquin.ortego@csic.es

[3]Island Ecology and Evolution Research Group, Institute of Natural Products and Agrobiology (IPNA-CSIC), La Laguna, Tenerife, Canarias, Spain

Received November 6, 2020
Accepted February 17, 2021

Although the pervasiveness of intraspecific wing-size polymorphism and transitions to flightlessness have long captivated biologists, the demographic outcomes of shifts in dispersal ability are not yet well understood and have been seldom studied at early stages of diversification. Here, we use genomic data to infer the consequences of dispersal-related trait variation in the taxonomically controversial short-winged (*Chorthippus corsicus corsicus*) and long-winged (*Chorthippus corsicus pascuorum*) Corsican grasshoppers. Our analyses revealed lack of contemporary hybridization between sympatric long- and short-winged forms and phylogenomic reconstructions supported their taxonomic distinctiveness, rejecting the hypothesis of intraspecific wing polymorphism. Statistical evaluation of alternative models of speciation strongly supported a scenario of Pleistocene divergence (<1.5 Ma) with ancestral gene flow. According to neutral expectations from differences in dispersal capacity, historical effective migration rates from the long- to the short-winged taxon were threefold higher than in the opposite direction. Although populations of the two taxa present a marked genetic structure and have experienced parallel demographic histories, our coalescent-based analyses suggest that reduced dispersal has fueled diversification in the short-winged *C. c. corsicus*. Collectively, our study illustrates how dispersal reduction can speed up geographical diversification and increase the opportunity for allopatric speciation in topographically complex landscapes.

KEY WORDS: Asymmetric gene flow, dispersal reduction, geographical diversification, Pleistocene speciation, speciation with gene flow, transitions to flightlessness.

Introduction

Dispersal polymorphism, wing-size polymorphism in particular, is a notorious attribute of numerous insect groups that has long fascinated ecologists and evolutionary biologists (Harrison 1980; Roff 1994). Dispersive phenotypes can confer an important advantage to colonize new habitats under changing environmental conditions (Simmons & Thomas 2004; Hochkirch & Damerau 2009) and favour population persistence in unstable habitats (Roff 1994). However, dispersal can be maladaptive under certain ecological settings (e.g., strong habitat isolation, windy alpine environments, etc.) and the production and maintenance of the flight apparatus is costly (Darwin, 1859; Harrison 1980; Waters et al. 2020). For these reasons, wing-size polymorphism has been often hypothesized to be maintained by a trade-off between dispersal benefits and investment in reproduction (Harrison 1980; Roff 1990; Wagner & Liebherr 1992; Zera & Denno 1997). Beyond intraspecific temporal and spatial variation in the proportion of long-winged forms resulted from either genetic polymorphism or phenotypic plasticity, transitions to flightlessness are common in Pterygota (winged) insects and other organism groups (Roff 1994; Kitson et al. 2018) and reversal from flightless to volant phenotypes might not be rare (Whiting et al. 2003; Zeng et al. 2020). Some studies have captured this evolutionary process at

*This article corresponds to J. Fenker et al. 2021. Digest: Dispersal reduction drives rapid diversification in alpine grasshoppers. Evolution. https://doi.org/10.1111/evo.14296

play, identifying steep or gradual clines in wing-size variation linked to ecological transitions that are often accompanied by disruption of gene flow (e.g., Dhuyvetter et al. 2007; Hendrickx et al. 2015; Dussex et al. 2016; Van Belleghem et al. 2018; McCulloch et al. 2019). However, detailed inferences on the tempo and mode of speciation and the magnitude and direction of intra- and interspecific gene flow are still needed to better understand the demographic consequences of evolutionary transitions in dispersal strategies (Van Belleghem et al. 2018; Waters et al. 2020).

The difficulty to ascribe short- and long-winged individuals to either a single polymorphic taxon or to distinct/incipient species with unimodal dispersive morphs has often led to taxonomic uncertainties, particularly when the two forms do not occur syntopically and, thus, reproductive isolation cannot be assessed in natural populations (Yue et al. 2014; Hendrickx et al. 2015; Veale et al. 2018). Distinguishing between these alternative scenarios is not only of great taxonomic importance but also critical to identify biological systems well-suited for the study of the demographic processes accompanying dispersal transitions (e.g., Ikeda et al. 2012; Vogler & Timmermans 2012; Van Belleghem et al. 2018). This can provide key information about the consequences of flightlessness on population subdivision and the magnitude and direction of gene flow, as these demographic processes can be readily compared between lineages representing incipient stages of the speciation process that differ in terms of dispersal ability but share common life-histories (e.g., McCulloch et al. 2019; Waters et al. 2020).

Orthoptera—crickets and grasshoppers—are among the most prominent wing polymorphic organisms (Simmons & Thomas 2004; Hochkirch & Damerau 2009) and transitions to flightlessness have occurred independently and repeatedly in many clades (Roff 1994). A paradigmatic example of taxonomic uncertainty linked to wing-size variation is the case of the Corsican grasshopper, which currently encompasses two subspecies (Cigliano et al. 2020): the short-winged *Chorthippus corsicus corsicus* (Chopard 1924) and the long-winged *Chorthippus corsicus pascuorum* (Chopard 1924) (Orthoptera: Acrididae; subgenus *Glyptobothrus*). Whereas both sexes of *C. c. pascuorum* are macropterous (i.e., long winged), males of *C. c. corsicus* are brachypterous (i.e., short winged) and females squamipterous (i.e., with considerably reduced or vestigial wings) (Braud et al. 2002). These two taxa were originally described as full species (Chopard 1924) and have experienced since then several changes in their taxonomic status based on subtle similarities and differences in morphology and courtship behaviour, including synonymization (Ragge & Reynolds 1998), re-elevation to their original full species rank (Voisin 2003), and downgrade to their current subspecific level (Defaut 2014; see Cigliano et al. 2020 for details on their taxonomic history). The two putative taxa present similar phenologies and ecological preferences for montane and alpine xeric open habitats dominated by thorny and dwarf shrub formations, with most of their populations located at elevational ranges between 1000 and 1800 m (Massa 1994; Braud et al. 2002). However, their distributions are parapatric, with *C. c. corsicus* being distributed in the northern half of Corsica and *C. c. pascuorum* occupying identical habitats in the southern half of the island (Massa 1994). The distributions of the two taxa overlap at the centre of Corsica, with a single known sympatric population where the two forms co-occur (Pfau 1984; Massa 1994). This raises the question on whether there is a single-wing polymorphic species with the co-occurrence of the two forms in at least one panmictic population (Roff 1990; Simmons & Thomas 2004; Hochkirch & Damerau 2009) or if, rather, they are independently evolving entities representing a transition between two dispersal phenotypes (Waters et al. 2020).

Here, we employ genomic data to shed light on the taxonomic status and demographic history of the Corsican grasshopper. In a first step, we reconstructed the phylogenomic relationships among populations of the two morphs to determine whether they correspond to a single-wing polymorphic taxon or to two independently evolving lineages (i.e., species) with unimodal phenotypes. Our analyses provided strong support for the taxonomic distinctiveness of long- and short-winged forms, rejecting the hypothesis of intraspecific wing polymorphism. In a second step, we performed a comprehensive suite of analyses to determine whether the two taxa are reproductively isolated, infer the tempo and mode of speciation, and analyse the demographic outcomes of wing-size reduction. Specifically, we used Bayesian clustering analyses to determine the genetic ancestry of individuals and test the hypothesis of contemporary hybridization (i.e., presence of F1 or F2 hybrids) in the only sympatric population where the two taxa co-occur. Then, we applied a coalescent-based approach to evaluate alternative models of speciation and lineage diversification and estimate demographic parameters under the most supported scenarios (Roux et al. 2016; Thome & Carstens 2016). We used these inferences to test two hypotheses about the consequences of dispersal-trait divergence: (i) differences in dispersal ability led to asymmetric gene flow from the long- to the short-winged taxon (Dussex et al. 2016); (ii) dispersal limitation (i.e., flightlessness) has diminished interpopulation migration rates, increased genetic structure and, ultimately, fueled geographical diversification in the short-winged taxon (Ikeda et al. 2012; Waters et al. 2020).

Materials and Methods

POPULATION SAMPLING

We sampled populations of *Chorthippus* (*Glyptobothrus*) *corsicus corsicus* and *Chorthippus* (*Glyptobothrus*) *corsicus pascuorum* from Corsica (France) (Table 1 and Fig. 1). Although

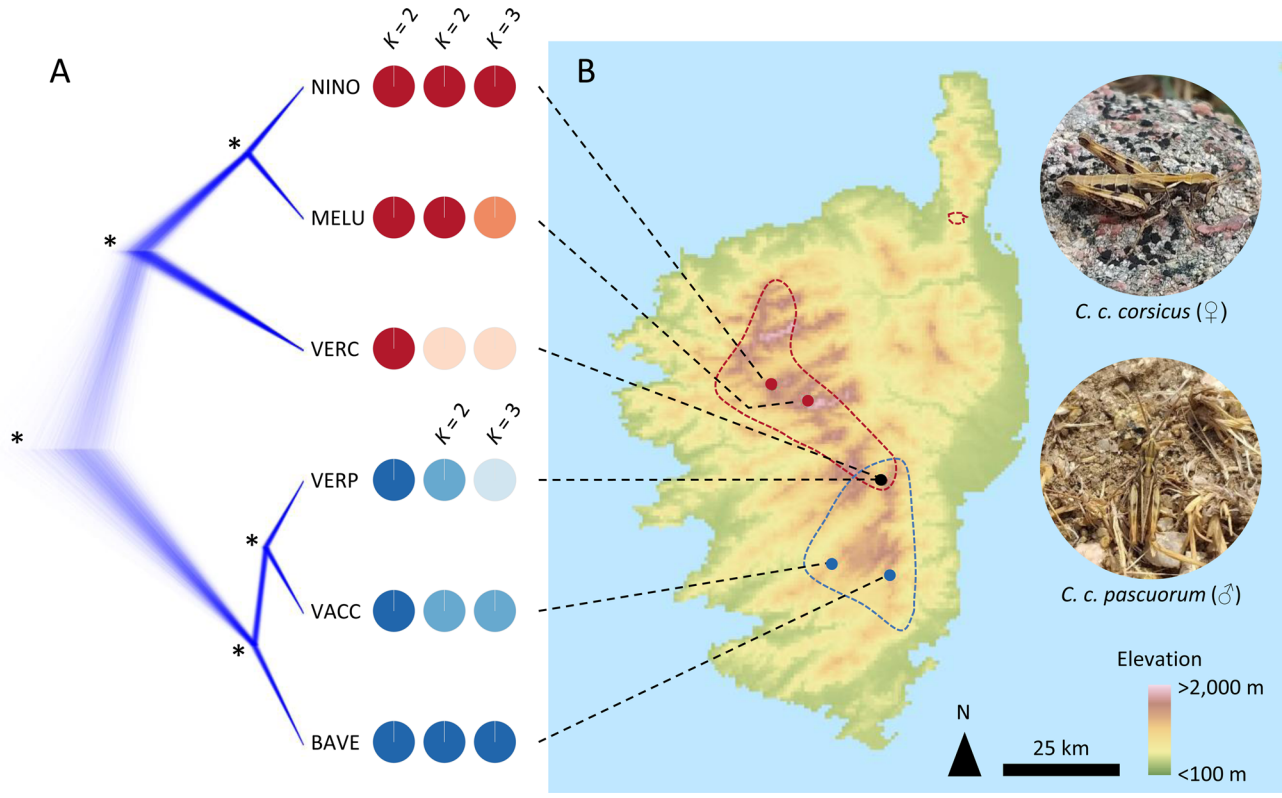

Figure 1. **(A) Phylogenetic relationships among populations of *Chorthippus corsicus corsicus* and *C. c. pascuorum* as inferred by SNAPP (4746 SNPs) and their genetic assignments based on the Bayesian clustering method implemented in the program STRUCTURE (pie charts). Asterisks on SNAPP tree mean fully supported nodes. STRUCTURE analyses were run including all populations of the two taxa (8764 SNPs; left pie charts) and independently for populations of *C. c. corsicus* (13,060 SNPs) and *C. c. pascuorum* (14,730 SNPs) (middle and right pie charts). (B) Map shows the geographical location of sampling sites (dots) and approximate distributions (dotted lines; based on Massa 1994) of *C. c. corsicus* (in red) and *C. c. pascuorum* (in blue). A black dot indicates the locality (Col de Verde) where the two taxa co-occur. Panel B includes a picture of the short-winged *C. c. corsicus* (top, female from Lac de Nino) and the long-winged *C. c. pascuorum* (bottom, male from Col de la Vaccia) (pictures by Joaquín Ortego). Population codes as described in Table 1.**

these two taxa are currently recognized as subspecies (Cigliano et al. 2020), they were originally described as distinct species (Chopard 1924) and our present analyses support that their full-species status should be restored (see "Conclusions" section). For this reason, hereafter, we treat the two taxa as different species but maintain their currently accepted designations (i.e., *C. c. corsicus* and *C. c. pascuorum*) pending their respective status to be formally updated. We used occurrence records available in the literature to design sampling and collect specimens from populations representative of their respective distribution ranges (Chopard 1924; Pfau 1984; Massa 1994; Braud et al. 2002), with special interest in the only locality (Col de Verde) where the two taxa are known to co-occur (Pfau 1984; Table 1 and Fig. 1). Specimens of *Chorthippus* (*Glyptobothrus*) *brunneus brunneus* (Thunberg, 1815) collected from Sardinia (Italy; Table 1) were used as outgroup in phylogenomic analyses and ABBA/BABA tests. We registered spatial coordinates using a Global Positioning System and preserved whole specimens at −20°C in 1500 μL 96% ethanol. Further details on sampling locations are provided in Table 1.

GENOMIC LIBRARY PREPARATION AND PROCESSING

We used NucleoSpin Tissue (Macherey-Nagel, Düren, Germany) kits to extract and purify DNA from a hind leg of each individual. We processed genomic DNA into one genomic library using the double-digestion restriction-site associated DNA sequencing procedure (ddRAD-seq) described in Peterson et al. (2012). In brief, we digested DNA with the restriction enzymes MseI and EcoRI (New England Biolabs, Ipswich, MA, USA) and ligated Illumina adaptors, including unique 7-bp barcodes, to the digested fragments of each individual. We pooled ligation products and size selected them between 475 and 580 bp with a Pippin Prep instrument (Sage Science, Beverly, MA, USA). We amplified the fragments by PCR with 12 cycles using the iProofTM High-Fidelity DNA Polymerase (BIO-RAD, Veenendaal, Netherlands) and sequenced the library in a single-read 150-bp lane on an Illumina HiSeq2500 platform at The Centre for Applied Genomics (Toronto, ON, Canada). Raw sequences were demultiplexed and preprocessed using STACKS version 1.35 (Catchen et al. 2013) and assembled using PYRAD version 3.0.66 (Eaton 2014). Methods

Table 1. Locality, region and country, code, number of genotyped individuals (*n*), latitude, longitude, elevation, and population genetic statistics (π, Tajima's D, and Fu's F_S) for each sampled taxon and population.

Taxon	Locality	Region (country)	Code	*n*	Latitude	Longitude	Elevation	π	Tajima's D	Fu's F_S
Chorthippus corsicus corsicus	Lac de Nino	Corsica (France)	NINO	8	42.256340	8.937995	1750	0.0048	−1.4240	−0.4534
Chorthippus corsicus corsicus	Lac de Melu	Corsica (France)	MELU	8	42.219566	9.024962	1540	0.0046	−1.0597	−0.5630
Chorthippus corsicus corsicus	Col de Verde	Corsica (France)	VERC	8	42.026210	9.204547	1480	0.0032	−0.9296	−0.9224
Chorthippus corsicus pascuorum	Col de Verde	Corsica (France)	VERP	8	42.027234	9.206082	1490	0.0040	−0.7296	−0.9607
Chorthippus corsicus pascuorum	Col de la Vaccia	Corsica (France)	VACC	8	41.824002	9.084002	1190	0.0035	−1.0641	−1.3567
Chorthippus corsicus pascuorum	Col de Bavella	Corsica (France)	BAVE	8	41.797365	9.223656	1220	0.0057	−1.2309	−1.8497
Chorthippus brunneus brunneus	Gennargentu	Sardinia (Italy)	CBRU	5	39.933750	9.179380	800	-	-	-

S1 provides all details on sequence assembling and data filtering. Unless otherwise indicated (see PCA and BPP analyses), all downstream analyses were performed using datasets of unlinked SNPs (i.e., a single SNP per RAD locus) obtained with PYRAD considering a clustering threshold of sequence similarity of 0.85 ($W_{clust} = 0.85$) and discarding loci that were not present in at least 50 % individuals ($minCov = 50\%$).

QUANTIFYING GENETIC STRUCTURE

We analysed population genetic structure and admixture using the Bayesian Markov Chain Monte Carlo (MCMC) clustering method implemented in the program STRUCTURE version 2.3.3 (Pritchard et al. 2000). We conducted STRUCTURE analyses hierarchically, initially analysing data from all populations and the two taxa jointly and, subsequently, running independent analyses for subsets of populations assigned to the same genetic cluster in the previous hierarchical level analysis (Janes et al. 2017; Pritchard et al. 2000). We ran STRUCTURE with 200,000 MCMC cycles after a burn-in step of 100,000 iterations, assuming correlated allele frequencies and admixture (Pritchard et al. 2000). We performed 15 independent runs for each value of K genetic clusters, where K ranged from 1 to $n + 1$ for each data set of n populations, to estimate the most likely number of clusters. We retained the ten runs having the highest likelihood for each value of K and checked that all retained replicates reached a similar solution in terms of individual's probabilities of assignment to each genetic cluster (q-values; Gilbert et al. 2012). As recommended by Gilbert et al. (2012) and Janes et al. (2017), we used two statistics to interpret the most likely number of genetic clusters (K): log probabilities of $Pr(X|K)$ (Pritchard et al. 2000) and ΔK (Evanno et al. 2005). These statistics were calculated using STRUCTURE HARVESTER (Earl & vonHoldt 2012). We used the Greedy algorithm in CLUMPP version 1.1.2 to align multiple runs of STRUCTURE for the same K value (Jakobsson & Rosenberg 2007) and DISTRUCT version 1.1 (Rosenberg 2004) to visualize as bar plots the individual's probabilities of population membership. Complementary to Bayesian clustering analyses, we performed principal component analyses (PCA) as implemented in the R version 3.3.2 (R Core Team 2020) package *adegenet* (Jombart 2008). Before running PCAs, we replaced missing data (∼32%) by the mean frequency of the corresponding allele estimated across all samples (Jombart 2008).

PHYLOGENOMIC INFERENCE

First, we reconstructed the phylogenetic relationships among taxa and populations using two coalescent methods, the Bayesian model implemented in SNAPP version 1.3 (Bryant et al. 2012) and the quartet-based approach implemented in SVDQUARTETS (Chifman & Kubatko 2014). Second, we used TREEMIX version 1.12 to assess the potential presence and direction of gene flow

between nonsister lineages that could distort tree topology (Pickrell & Pritchard 2012). Finally, we used the multispecies coalescent model implemented BPP version 4.0 to estimate divergence times (Flouri et al. 2018).

Snapp

We ran SNAPP as implemented in BEAST version 2.4.1 (Bouckaert et al. 2014). Due to large computational demands of this program, we only included in the analyses three individuals per population. We selected the three individuals from each population that had the lowest proportion of missing data and, thus, retained the highest number of SNPs. The resulting dataset included 4746 unlinked SNPs shared across tips (i.e., populations). Initially, we ran pilot analyses with different values of the shape (α) and inverse scale (β) parameters of the gamma prior distribution ($\alpha = 2$, $\beta = 200$; $\alpha = 2$, $\beta = 2000$; $\alpha = 2$, $\beta = 20{,}000$) for the population size parameter (θ), leaving default settings for all other parameters. These analyses yielded the same topology (not shown) and only results for the intermediate prior for theta are presented ($\alpha = 2$, $\beta = 2000$). We used different starting seeds to perform two independent replicate runs of >2 million generations sampled every 1000 steps (i.e., >2000 retained genealogies). We used TRACER version 1.4 to examine log files and check stationarity and convergence of the chains and confirm that effective sample sizes (ESS) for all parameters were >200. We removed 10% of trees as burn-in and combined tree and log files for replicated runs using LOGCOMBINER version 2.4.1. We used TREEANNOTATOR version 1.8.3 to obtain maximum credibility trees, TREESETANALYSER version 2.4.1 to identify trees contained in the 95% highest posterior density (HPD) set, and DENSITREE version 2.2.1 (Bouckaert 2010) to display the full set of trees.

Svdquartets

We ran SVDQUARTETS as implemented in PAUP* version 4.0a152 (Swofford 2002). Phylogenetic trees in SVDQUARTETS were constructed by exhaustively evaluating all possible quartets from the dataset (8334 unlinked SNPs, including the outgroup) and uncertainty in relationships was quantified using 1000 bootstrapping replicates. Five individuals of *C. brunneus brunneus* were used as outgroup (Table 1). Given the low computational burden of SVDQUARTETS in comparison with SNAPP, in this case we included all genotyped individuals in the analysis.

Treemix

First, we estimated a maximum-likelihood tree rooted with the outgroup *C. brunneus brunneus*. Then, we tested a range of migration events (*m* from 0 to 5) and used an information-theoretic model selection approach based on the Akaike's information criterion (AIC) to determine the model best fitting the data (Burnham & Anderson 2002). The input dataset (allele counts; Pickrell & Pritchard 2012) was based on 2444 unlinked SNPs shared across all tips (i.e., all ingroup populations plus the outgroup). We assumed independence of all SNPs and used a window size of one SNP ($k = 1$).

Bpp

The phylogenetic tree inferred using SVDQUARTETS, SNAPP, and TREEMIX was fitted as the fixed topology in BPP analyses to estimate divergence times (option A00). Unlike SNP-based analyses implemented in SNAPP, SVDQUARTETS, and TREEMIX, BPP uses whole ddRAD-seq loci. The *.loci* file from PYRAD was edited, converted into a BPP input file, and filtered using custom R scripts (J-P. Huang, https://github.com/airbugs/; for details, see Huang et al. 2020). As all sequences do not have the same length due to insertion-deletion polymorphisms (indels) at some loci, we trimmed them to 110 bp and excluded loci that were not represented in at least one individual per population (i.e., as in SNAPP, loci with missing taxa/populations were removed). This resulted in a BPP input file containing 5640 loci. We applied an automatic adjustment of fine-tune parameters and set the diploid option to indicate that the input sequences are unphased (Flouri et al. 2018). To ensure the convergence of the runs (ESS > 200), two independent replicate analyses were run for 200,000 generations, sampling every 2 generations, after a burn-in of 20,000 generations. We estimated divergence times using the equation $\tau = 2\mu t$, where τ is the divergence in substitutions per site estimated by BPP, μ is the per site mutation rate per generation, and t is the absolute divergence time in years (Walsh 2001). We considered the mutation rate per site per generation of 2.8×10^{-9} estimated for *Drosophila melanogaster* (Keightley et al. 2014), which is similar to the spontaneous mutation rate estimated for the butterfly *Heliconius melpomene* (2.9×10^{-9}; Keightley et al. 2015).

TESTS OF INTROGRESSION

We used four-taxon ABBA/BABA tests based on the *D*-statistic to infer whether some specific populations from one taxon (*C. c. corsicus* or *C. c. pascuorum*) show a disproportionally higher signal of introgression from the other taxon (Durand et al. 2011). Assuming that the sister populations P1 and P2 diverged from taxon P3 and an outgroup species O, the *D*-statistic is used to test the null hypothesis of no introgression ($D = 0$) between P3 and P1 or P2. *D*-values significantly different from zero indicate gene flow between P1 and P3 ($D < 0$) or between P2 and P3 ($D > 0$). We assigned to P1 and P2 two populations from one taxon, to P3 one population of the other taxon, and to O the outgroup (*C. brunneus brunneus*). We performed ABBA/BABA tests considering all possible population combinations (see Supporting information Table S1). Tests were run in PYRAD with 1000 bootstrap replicates to obtain the standard deviation of the *D*-statistic and significance levels (Eaton & Ree 2013).

Table 2. Comparison of alternative models of (A) speciation and (B, C) intraspecific divergence for *Chorthippus corsicus corsicus* and *C. c. pascuorum* tested using FASTSIMCOAL2, with their respective best supported scenario highlighted in bold.

Model	lnL	*k*	AIC	ΔAIC	ω_i
(A) Speciation					
(1) SI	−6056.22	3	12,118.45	34.33	0.00
(2) IM_S	−6042.84	4	12,093.68	9.57	0.01
(3) IM_A	−6038.25	5	12,086.50	2.39	0.21
(4) AM_S	−6041.36	5	12,092.71	8.60	0.01
(5) **AM_A**	**−6036.06**	**6**	**12,084.11**	**0.00**	**0.68**
(6) SC_S	−6042.93	5	12,095.86	11.74	0.00
(7) SC_A	−6038.07	6	12,088.15	4.03	0.09
(B) Intraspecific divergence—*C. c. corsicus*					
(1) SI ((NINO, MELU), VERC)	−4454.55	6	8921.10	6.37	0.02
(2) IM_S ((NINO↔MELU)↔VERC)	−4450.69	8	8917.39	2.65	0.12
(3) IM_A ((NINO↔MELU)↔VERC)	−4449.05	10	8918.09	3.36	0.09
(4) SI + IM_S ((NINO↔MELU), VERC)	−4451.02	7	8916.04	1.30	0.24
(5) **SI + IM_A ((NINO↔MELU), VERC)**	**−4449.37**	**8**	**8914.74**	**0.00**	**0.47**
(6) SI + IM_S ((NINO, MELU)↔VERC)	−4453.78	7	8921.57	6.83	0.02
(7) SI + IM_A ((NINO, MELU)↔VERC)	−4451.83	8	8919.66	4.93	0.04
(C) Intraspecific divergence—*C. c. pascuorum*					
(1) SI ((VERP, VACC), BAVE)	−6110.81	6	12,233.62	1.12	0.23
(2) **IM_S ((VERP↔VACC)↔BAVE)**	**−6108.25**	**8**	**12,232.50**	**0.00**	**0.39**
(3) IM_A ((VERP↔VACC)↔BAVE)	−6109.72	10	12,239.44	6.93	0.01
(4) SI + IM_S ((VERP↔VACC), BAVE)	−6111.60	7	12,237.19	4.69	0.04
(5) SI + IM_A ((VERP↔VACC), BAVE)	−6110.83	8	12,237.66	5.15	0.03
(6) SI + IM_S ((VERP, VACC)↔BAVE)	−6110.39	7	12,234.78	2.27	0.13
(7) SI + IM_A ((VERP, VACC)↔BAVE)	−6109.08	8	12,234.15	1.65	0.17

Speciation models include scenarios of divergence in strict isolation (SI), isolation-with-migration (IM), ancestral migration (AM), and secondary contact (SC), the last three considering either symmetric (IM_S, AM_S, and SC_S) or asymmetric (IM_A, AM_A, and SC_A) gene flow. Models of intraspecific divergence consider alternative combinations of IM and SI scenarios, with the specific demes exchanging either symmetric or asymmetric gene flow (arrows) indicated in parentheses (population codes as described in Table 1).

lnL, maximum likelihood value of the model; *k*, number of parameters in the model; AIC, Akaike's information criterion value; ΔAIC, difference in AIC value from that of the strongest model; ω_i, AIC weight.

TESTING ALTERNATIVE DEMOGRAPHIC MODELS

In a first step, we tested alternative models of speciation that considered two demes corresponding with *C. c. corsicus* and *C. c. pascuorum*. As the two taxa were supported as reciprocally monophyletic by phylogenomic analyses (see Results section), individuals from the three genotyped populations of each taxon were pooled together. Specifically, we tested a model of speciation in strict isolation (SI) and alternative models incorporating interspecific gene flow including isolation-with-migration (IM), ancestral migration (AM), and secondary contact (SC). In turn, the three gene flow models considered either symmetrical or asymmetrical migration matrices connecting the two taxa (Table 2). In a second step, we tested alternative models of intraspecific population divergence focusing on each taxon separately. These models included scenarios of divergence in SI, IM, and alternative combinations of SI and IM scenarios in which only specific demes exchange either symmetric or asymmetric gene flow (see Table 2). The number of parameters of each tested model is detailed in Table 2.

We estimated the composite likelihood of the observed data given a specified model using the site-frequency spectrum (SFS) and the simulation-based approach implemented in FASTSIMCOAL2 (Excoffier et al. 2013). As a reference genome is not available, we calculated folded joint SFS and considered a single SNP per locus to avoid the effects of linkage disequilibrium. Because we did not include invariable sites in the SFS, we fixed the effective population size for one of the demes (*C. c. corsicus* for speciation models and populations from Col de Verde for intraspecific divergence models of *C. c. corsicus* and *C. c. pascuorum*) to enable the estimation of other parameters in FASTSIMCOAL2 (Excoffier et al. 2013). The effective population size fixed in the model was calculated from the level of nucleotide diversity (π) and estimates of mutation rate per site per generation (μ; 2.8×10^{-9}; Keightley et al. 2014). Nucleotide

diversity (π) was estimated from polymorphic and nonpolymorphic loci using DNASP version 6.12.03 (Rozas et al. 2017). To remove all missing data for the calculation of the joint SFS, minimize errors with allele frequency estimates and maximize the number of variable SNPs retained, each population group was down sampled to 50% of individuals in speciation models (i.e., 12 individuals per taxon; Table 1) and 62.5% of individuals for intraspecific divergence models (i.e., 5 individuals per population; Table 1) using the *easySFS.py* script (I. Overcast, https://github.com/isaacovercast/easySFS). Final site frequency spectra contained 3857 variable SNPs for speciation models and 2784 and 3545 variable SNPs for intraspecific divergence models of *C. c. corsicus* and *C. c. pascuorum*, respectively.

Each model was run 100 replicated times considering 100,000-250,000 simulations for the calculation of the composite likelihood, 10-40 expectation-conditional maximization cycles, and a stopping criterion of 0.001 (Excoffier et al. 2013). We used an information-theoretic model selection approach based on the AIC to determine the probability of each model given the observed data (Burnham & Anderson 2002). After the maximum likelihood was estimated for each model in every replicate, we calculated the AIC scores as detailed in Thome & Carsterns (2016). AIC values for each model were rescaled (ΔAIC) calculating the difference between the AIC value of each model and the minimum AIC obtained among all competing models (i.e., the best model has $\Delta AIC = 0$). Point estimates of the different demographic parameters for the best supported model were selected from the run with the highest maximum composite likelihood. Finally, we calculated confidence intervals of parameter estimates from 100 parametric bootstrap replicates by simulating SFS from the maximum composite likelihood estimates and re-estimating parameters each time (Excoffier et al. 2013).

ANALYSES OF GENETIC DIVERSITY AND CHANGES OF Ne THROUGH TIME

First, we used DNASP to calculate nucleotide diversity (π) and ARLEQUIN version 3.5 (Excoffier et al. 2005) to perform Tajima´s D (Tajima 1989) and Fu's F_S (Fu 1997) tests of neutrality for each population. Significance of neutrality tests was assessed using 10,000 coalescent simulations (Excoffier et al. 2005). Second, we inferred changes in effective population size (N_e) through time for each population using the program STAIRWAY PLOT, which implements a flexible multiepoch demographic model based on the SFS that does not require whole-genome sequence data or reference genome information (Liu & Fu 2015). Each population was down sampled to 75% of individuals (six individuals per population; Table 1) using the *easySFS.py* script as described above for FASTSIMCOAL2 analyses. We ran STAIRWAY PLOT considering the 1-year generation time of *Glyptobothrus* grasshoppers (Laiolo et al. 2013; Cárdenas et al. 2017), assuming a mutation rate per site per generation of 2.8×10^{-9} (Keightley et al. 2014), and performing 200 bootstrap replicates to estimate 95% confidence intervals (Liu & Fu 2015).

Results

GENOMIC DATA AND POPULATION GENETIC STATISTICS

The average number of reads retained per individual after the different quality filtering steps was 2,600,861 (range = 795,629-3,631,280 reads; Supporting information Fig. S1). On average, this represented 77% (range = 60-80%) of the total number of reads recovered for each individual (Supporting information Fig. S1). After filtering loci considering a *minCov* = 50% (see Methods S1), the dataset including the two taxa contained 8764 variable loci with a mean of 10.06 SNPs per RAD locus. The datasets for *C. c. corsicus* and *C. c. pascuorum* contained 13,060 (mean number of SNPs per RAD locus = 7.43) and 14,730 (mean number of SNPs per RAD locus = 5.59) loci, respectively.

QUANTIFYING GENETIC STRUCTURE

STRUCTURE analyses (Pritchard et al. 2000) based on all populations and the two taxa identified that the most likely number of clusters was $K = 2$ according to the ΔK criterion (Evanno et al. 2005), but $LnPr(X|K)$ reached a plateau at $K = 3$ (Supporting information Fig. S2A). For $K = 2$, the two genetic clusters separated *C. c. corsicus* from *C. c. pascuorum* and the probabilities of assignment inferred by STRUCTURE revealed no signatures of genetic admixture between the two taxa in any population (q-values = 1 for all individuals; Fig. 1A and Supporting information Fig. S3A). STRUCTURE analyses for $K = 3$ split the three populations of *C. c. corsicus* into two clusters, one including the northernmost populations (NINO and MELU) and another including the geographically more isolated population from Col de Verde (VERC) (Fig. 1A and Supporting information Fig. S3A). Hierarchical STRUCTURE analyses ran independently for populations of the two taxa revealed a marked genetic structure. STRUCTURE analyses focused on populations of *C. c. corsicus* identified that the most likely number of clusters was $K = 2$ according to the ΔK criterion, but $LnPr(X|K)$ reached a plateau at $K = 3$ (Supporting information Fig. S2B). As shown for global analyses, STRUCTURE analyses for $K = 2$ split the geographically isolated population from Col de Verde (VERC) and the two northernmost populations (NINO and MELU) (Fig. 1A and Supporting information Fig. S3B). In turn, these last two populations separated into two genetic clusters for $K = 3$ (Fig. 1A and Supporting information Fig. S3B). STRUCTURE analyses focused on populations of *C. c. pascuorum* identified that the most likely number of clusters was $K = 3$ according to the ΔK criterion and $LnPr(X|K)$ reached a plateau for the same K value (Fig. S2C). Analyses for $K = 2$

separated the population BAVE from VERP and VACC, which in turn split into two well-defined genetic clusters for $K = 3$ (Fig. 1A and Supporting information Fig. S3C). Thus, all populations of the two taxa were fully assigned to different genetic clusters with no signatures of genetic admixture (q values $= 1$ for all individuals; Fig. 1A and Supporting information Fig. S3).

PCA (Jombart 2008) were consistent with the results yielded by STRUCTURE at different hierarchical levels (Supporting information Fig. S4). Global analyses including all populations from the two taxa separated *C. c. corsicus* and *C. c. pascuorum* along the first principal component (PC1), whereas the second principal component (PC2) separated the geographically isolated population from Col de Verde (VERC) from the two northernmost populations (NINO and MELU) of *C. c. corsicus* (Supporting information Fig. S4A). PCA ran independently for populations of the two taxa separated their respective populations in three different genetic clusters along PC1 and PC2, supporting the marked genetic structure inferred by STRUCTURE (Supporting information Fig. S4B and C). PCA run considering SNP datasets without missing data (*minCov* = 100%) yielded qualitatively analogous results, although individuals within the identified clusters tended to show a higher dispersion due to only highly conserved loci shared across all individuals, populations and taxa are retained in SNP matrices without missing data (Supporting information Fig. S4D-F).

PHYLOGENOMIC INFERENCE

Phylogenomic analyses based on SNAPP (Bryant et al. 2012; Fig. 1A) and SVDQUARTETS (Chifman & Kubatko 2014; Supporting information Fig. S5) yielded the same topology and supported that populations of *C. c. corsicus* and *C. c. pascuorum* are reciprocally monophyletic. Populations and taxa split in the same order as in the hierarchical analyses with STRUCTURE (see Fig. 1A and previous section) and phylogenetic relationships among them were fully supported by both SNAPP (posterior probabilities = 1; Fig. 1A) and SVDQUARTETS analyses (bootstrap support = 100%; Supporting information Fig. S5). TREESETANALYSER showed that a single topology was contained in the 95% HPD tree set (Fig. 1A). TREEMIX analyses (Pickrell & Pritchard 2012) retrieved the same topology than SNAPP and SVDQUARTETS and showed that a population graph model with no migration is statistically indistinguishable (ΔAIC < 0.4) or more supported than models with one or more migration events, indicating no evidence for postdivergence gene flow between nonsister lineages (Supporting information Table S2 and Fig. S6).

Assuming divergence in SI (i.e., lack of postdivergence gene flow), a genomic mutation rate of 2.8×10^{-9} per site per generation (Keightley et al. 2014) and a 1-year generation time, BPP analyses (Flouri et al. 2018) estimated that the two taxa diverged from a common ancestor at the beginning of the middle Pleistocene (ca. 0.68 Ma; Supporting information Fig. S7). The second oldest split involved the geographically isolated population from Col de Verde (VERC) and the two northernmost populations (NINO and MELU) of *C. c. corsicus*, which diverged at the mid of the middle Pleistocene (ca. 0.44 Ma; Supporting information Fig. S7). The rest of the populations diverged during the upper Pleistocene (ca. 0.11-0.02 Ma), with the most recent split involving the geographically close populations VACC and VERP from *C. c. pascuorum* (Supporting information Fig. S7).

TESTS OF INTROGRESSION

Most ABBA-BABA tests (Durand et al. 2011) were not significant, indicating that the signals of historical interspecific gene flow identified by FASTSIMCOAL2 analyses (see section "Testing alternative demographic models") are similar across populations (Supporting information Table S1). The only exceptions were some comparisons involving the populations VACC from *C. c. pascuorum* and NINO from *C. c. corsicus*. These populations, particularly VACC, tended to show higher levels of introgression than other populations from the same taxon, although this was not significant for all population combinations (Supporting information Table S1). Remarkably, sympatric populations from Col de Verde of either *C. c. corsicus* (VERC) or *C. c. pascuorum* (VERP) did not show disproportionately higher levels of genetic introgression in comparison with other populations (Supporting information Table S1).

TESTING ALTERNATIVE DEMOGRAPHIC MODELS

FASTSIMCOAL2 analyses (Excoffier et al. 2013) showed that the most supported model of speciation was the one considering AM with asymmetric gene flow (Fig. 2 and Table 2). Considering a 1-year generation time, the split between *C. c. corsicus* and *C. c. pascuorum* was estimated to take place during the early Pleistocene (ca. 1.3 Ma; Calabrian stage; Table 3) and ancestral gene flow between the two taxa interrupted at the end of the last glacial period (ca. 30 ka). Effective migration rate per generation (2 Nm) from *C. c. pascuorum* to *C. c. corsicus* was threefold higher than in the opposite direction and such differences were statistically significant (i.e., 95% confidence intervals did not overlap; Table 3). Accordingly, posthoc testing of an AM model with unidirectional gene flow from *C. c. pascuorum* to *C. c. corsicus* revealed that it was statistically undistinguishable from a model considering bidirectional and asymmetric gene flow (ΔAIC = 0.05), whereas an AM model fitting unidirectional gene flow from *C. c. corsicus* to *C. c. pascuorum* was very poorly supported (ΔAIC = 8).

The most supported model of intraspecific divergence for *C. c. corsicus* was a mixed scenario considering divergence in SI of VERC population and isolation with asymmetric gene flow (IM) for the nearby populations NINO and MELU (Fig. 2 and

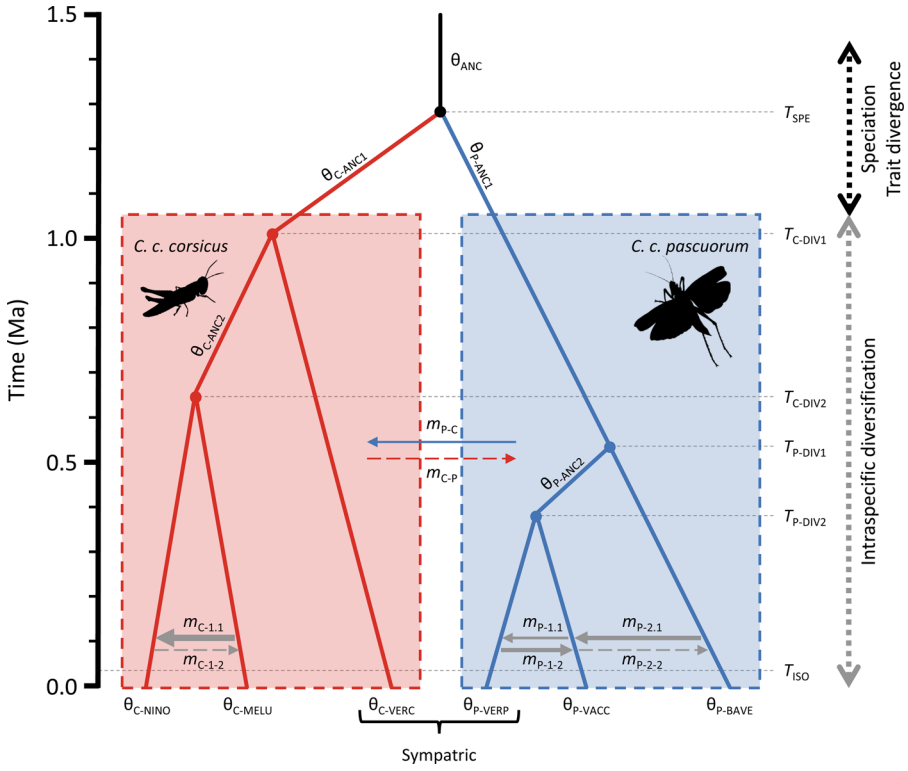

Figure 2. Schematic diagram of the most supported scenario of speciation and intraspecific divergence for the short-winged *Chorthippus corsicus corsicus* (left, in red) and the long-winged *C. c. pascuorum* (right, in blue) as inferred from coalescent simulations with FASTSIMCOAL2. Parameters include mutation-scaled ancestral and contemporary effective population sizes (θ), effective migration rates per generation (*m*), and timing of speciation (T_{SPE}), interruption of interspecific gene flow (T_{ISO}), and population divergence (T_{DIV}). Point estimates yielded by FASTSIMCOAL2 were used to scale the different time events (*T*) (left axis) and effective migration rates per generation (*m*, proportional to arrow thickness, with dashed lines indicating estimates 2 Nm < 0.1). Demographic parameter values and confidence intervals are detailed in Table 3. Population codes as described in Table 1.

Table 2). This model estimated that the split of VERC took place in the early Pleistocene (ca. 1 Ma, Calabrian stage), whereas the divergence between the nearby MELU and NINO populations happened during the middle Pleistocene (ca. 0.65 Ma, Chibanian age) (Table 3 and Fig. 2). The most supported model of intraspecific divergence for *C. c. pascuorum* was an IM scenario with symmetric gene flow (Fig. 2 and Table 2). This model estimated that the two divergence events took place in the middle Pleistocene (Chibanian age; ca. 0.53 and 0.39 Ma for the earliest and most recent split, respectively; Table 3 and Fig. 2).

ANALYSES OF GENETIC DIVERSITY AND CHANGES OF Ne THROUGH TIME

Nucleotide diversity (π) ranged between 0.0032 and 0.0057 (Table 1). Tajima´s D and Fu's F_S tests were not significant in any population ($P > 0.1$), indicating that genomic variation does not depart from neutral expectations (Table 1). STAIRWAY PLOT analyses (Liu & Fu 2015) revealed that all analysed populations of the two taxa experienced parallel changes of N_e through time, undergoing severe demographic declines starting at the onset of the Holocene that have reduced their N_e by >99 % since the LGM (Fig. 3 and Supporting information Fig. S8).

Discussion

Genomic analyses supported the taxonomic distinctiveness of the short-winged *C. c. corsicus* and the long-winged *C. c. pascuorum*, rejecting the hypothesis of intraspecific wing polymorphism (Simmons & Thomas 2004; Hochkirch & Damerau 2009). In contrast to previous recent studies on other insects (e.g., stoneflies; McCulloch et al. 2019; beetles: Van Belleghem et al. 2018), our results point to a single evolutionary transition that is not apparently linked to an ecological shift or any contemporary environmental gradient. Considering that the vast majority of Pterygota insects with reduced or no wings have secondarily become flightless (Roff 1990) and most taxa within the subgenus *Glyptobothrus* are long winged (Cigliano et al. 2020), the divergence of *C. c. corsicus* and *C. c. pascuorum* most likely represents an evolutionary transition from a long- to a short-winged state (see also McCulloch et al. 2009 2019). Inferences from coalescent-based

Table 3. Parameters inferred from coalescent simulations with FASTSIMCOAL2 under the most supported scenario of (A) speciation and (B, C) intraspecific divergence for *Chorthippus corsicus corsicus* and *C. c. pascuorum*.

Parameter	Point estimate	Lower bound	Upper bound
(A) Speciation			
θ_{ANC}	835,961	669,238	733,847
θ_{COR}	1,325,651	-	-
θ_{PAS}	717,463	702,455	717,111
T_{SPE}	1,273,731	1,343,521	1,417,469
T_{ISO}	29,418	28,727	35,053
$m_{C\text{-}P}$	0.0407	0.0384	0.0447
$m_{P\text{-}C}$	0.1249	0.1223	0.1317
(B) Intraspecific divergence—*C. c. corsicus*			
$\theta_{C\text{-}ANC1}$	2,676,959	1,928,670	1,991,766
$\theta_{C\text{-}ANC2}$	380,347	435,142	456,854
$\theta_{C\text{-}NINO}$	1,042,681	953,397	982,958
$\theta_{C\text{-}MELU}$	625,513	581,588	604,512
$\theta_{C\text{-}VERC}$	565,064	-	-
$T_{C\text{-}DIV1}$	1,005,616	1,064,134	1,079,759
$T_{C\text{-}DIV2}$	654,038	620,772	643,038
$m_{C\text{-}1.1}$	0.3566	0.3420	0.3618
$m_{C\text{-}1.2}$	0.0001	0.0067	0.0161
(C) Intraspecific divergence—*C. c. pascuorum*			
$\theta_{P\text{-}ANC1}$	1,579,017	1,296,678	1,331,547
$\theta_{P\text{-}ANC2}$	628,857	482,436	535,203
$\theta_{P\text{-}VERP}$	708,547	-	-
$\theta_{P\text{-}VACC}$	476,179	443,081	455,092
$\theta_{P\text{-}BAVE}$	1,477,210	1,324,022	1,369,577
$T_{P\text{-}DIV1}$	528,773	505,146	522,546
$T_{P\text{-}DIV2}$	388,807	381,739	400,775
$m_{P\text{-}1.1}$	0.1613	0.1506	0.1650
$m_{P\text{-}1.2}$	0.2401	0.2384	0.2612
$m_{P\text{-}2.1}$	0.2551	0.2506	0.2686
$m_{P\text{-}2.2}$	0.0822	0.0837	0.0892

Table shows point estimates and lower and upper 95% confidence intervals for each parameter, which include mutation-scaled ancestral and contemporary effective population sizes (θ), effective migration rates per generation (m), and timing of speciation (T_{SPE}), interruption of interspecific gene flow (T_{ISO}), and population divergence (T_{DIV}). Parameters θ_{COR} and θ_{PAS} in the speciation model correspond to contemporary effective population sizes of *C. c. corsicus* and *C. c. pascuorum*, respectively. The rest of parameters are illustrated in Figure 2. Estimates of time are given in units of generations and migration rates (m) are presented as 2 Nm. Note that contemporary effective population sizes of *Chorthippus corsicus corsicus* (θ_{COR}) in the speciation model and for populations from Col de Verde of both *C. c. corsicus* ($\theta_{C\text{-}VERC}$) and *C. c. pascuorum* ($\theta_{P\text{-}VERP}$) were calculated from their respective levels of nucleotide diversity (π) and fixed in FASTSIMCOAL2 analyses to enable the estimation of other parameters (see the Materials and Methods section for further details).

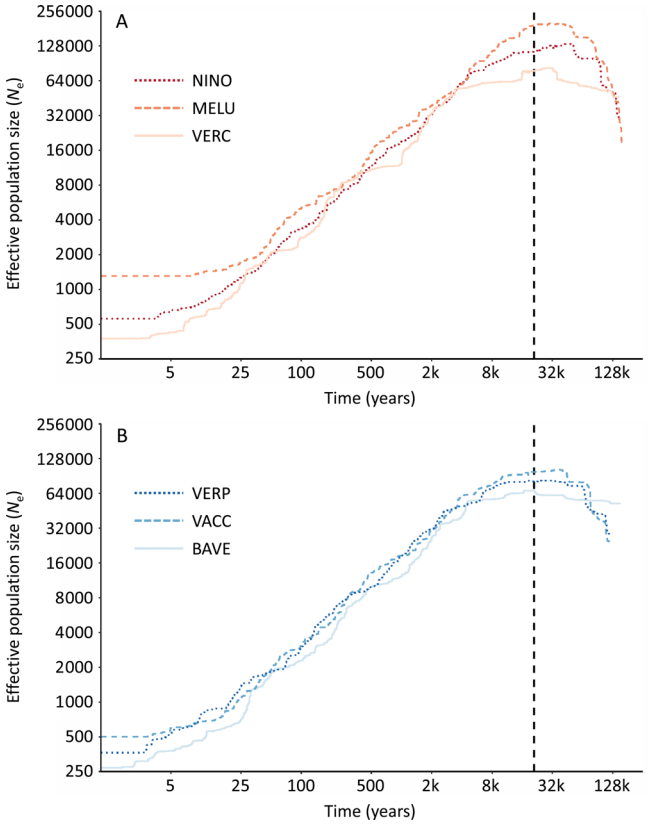

Figure 3. Demographic history of the studied populations of (A) *Chorthippus corsicus corsicus* and (B) *C. c. pascuorum* inferred using STAIRWAY PLOT. Panels show median effective population sizes (N_e) over time, estimated assuming a mutation rate of 2.8×10^{-9} and 1-year generation time (both axes in a logarithmic scale). Vertical dashed lines indicate the Last Glacial Maximum (LGM; ~21 ka BP). Population codes as described in Table 1.

analyses suggest that wing-size reduction can also have important demographic consequences at different stages along the speciation continuum, impacting both the direction and magnitude of interspecific gene flow and intraspecific rates of dispersal and geographical diversification (Waters et al. 2020).

DIVERGENCE WITH ASYMMETRIC GENE FLOW

Our model-based approach in FASTSIMCOAL2 revealed that the null scenario of divergence in SI was highly unlikely, strongly supporting a model of speciation with ancestral gene flow (Fig. 2). This finding is in agreement with several recent studies suggesting that gene flow might be a common phenomenon in early stages of the divergence (Hey 2006; Nosil 2008; Pinho & Hey 2010; Morales et al. 2017). However, it must be noted that a scenario of speciation with gene flow and a scenario of speciation in SI with SC are difficult to discern exclusively based on genomic data and the categorical rejection of speciation in strict allopatry requires external sources of evidence such as those provided by the biogeographical setting of divergence (e.g., the

presence/absence of geographical barriers) and/or functional genomics (Yang et al. 2017; see also Feder et al. 2013). The island of Corsica presents an extremely complex topography and its central and northern mountains were extensively glaciated during the coldest stages of the Pleistocene (Kuhlemann et al. 2005), providing a biogeographic scenario well-suited for allopatric divergence. Also, *C. c. corsicus* and *C. c. pascuorum* are patchily distributed taxa presenting a single known sympatric population at the centre of the island (Massa 1994). Thus, one possibility is that the two taxa initially diverged in strict allopatry, came into secondary contact shortly after (e.g., following demographic expansions), and exchanged genes for a certain period of time (Coyne & Orr 2004; Feder et al. 2013; Tonzo et al. 2020).

Divergence time estimates under the most supported model of speciation indicate that the two taxa most likely diverged at the end of the early Pleistocene (ca. 1.3-1.4 Ma; Fig. 2), which falls within the range of divergence times reported in previous studies for sister species in other recent radiations of grasshoppers (e.g., Carstens & Knowles 2007a; Scattolini et al. 2018; Huang et al. 2020). As expected, divergence times were considerably underestimated by BPP analyses (0.67-0.70 Ma) assuming speciation without postdivergence gene flow (Fig. 2). Estimates of divergence time yielded by BPP were similar to those obtained under the highly unsupported model of speciation in SI (T_{SPE}: 0.86-0.87 Ma), a scenario that also overestimated ancestral and contemporary effective population sizes in comparison with the best ranked model considering ancestral gene flow (see Supporting information Table S3). These results illustrate how key demographic parameters (i.e., effective population sizes and divergence times) can be severely biased when shared polymorphism is exclusively attributed to incomplete lineage sorting, highlighting the importance of modelling gene flow to obtain accurate inferences on both the tempo and mode of species formation (Leaché et al. 2014; Morales et al. 2017).

DEMOGRAPHIC CONSEQUENCES OF WING-SIZE REDUCTION

According to neutral expectations, our coalescent-based demographic analyses suggest that lower dispersal capacity has reduced gene flow and accelerated geographical diversification in the short-winged taxon (Waters et al. 2020; e.g., McCulloch et al. 2009). Statistical comparison of the likelihoods of alternative speciation models revealed that scenarios including asymmetrical gene flow were strongly favoured over those considering symmetrical migration (Table 2). Specifically, effective migration rate from *C. c. pascuorum* to *C. c. corsicus* was estimated to be threefold higher than in the opposite direction (Table 3). Such differences in ancestral effective migration rates per generation could be explained by the higher dispersal capacity of the long-winged *C. c. pascuorum* in comparison with the short-winged *C. c. corsicus*, which might have favoured that the former historically dispersed more frequently into the range of the latter (e.g., under changing environmental conditions) and this, ultimately, led to asymmetrical gene flow (Jacquemyn et al. 2012). These findings are congruent with the results from recent studies on the saltmarsh beetle (*Pogonus chalceus*), in which long- and short-winged ecotypes have repeatedly evolved in response to contrasting hydrological regimes (Dhuyvetter et al. 2007; Van Belleghem et al. 2018). These two ecotypes have not yet reached reproductive isolation and demographic models estimating contemporary gene flow in four spatial replicates revealed that, in three of them, effective migration rates were significantly higher from the long- to the short-winged ecotype than in the opposite direction (Van Belleghem et al. 2018). These results indicate that transitions to flightlessness probably lead to source-sink dynamics disproportionately impacting genetic drift in the less dispersive lineage, a scenario where the fixation of flightlessness, depending on the magnitude of gene flow, might require strong disruptive selection (Pinho & Hey 2010). In our specific case, estimated effective migration rates were well below the threshold (2 Nm∼1; Wright 1931) that would prevent divergence by genetic drift (Table 2) and, thus, are compatible with the initiation and completion of the speciation process even in absence of strong selection (Pinho & Hey 2010; Barton 2020).

Taxon-specific demographic analyses have also revealed older divergence times among populations of the short-winged *C. c. corsicus*, suggesting that limited dispersal capacity has contributed to reduce or disrupt gene flow and speed up geographical diversification in this taxon (Table 3 and Fig. 2). Despite the distances among sampled populations are fairly similar in the two taxa (Fig. 1), estimated divergence times were significantly older and interpopulation effective migration rates smaller (or absent) in the poor flyer *C. c. corsicus* than in the macropterous *C. c. pascuorum* (Table 3 and Fig. 2). The magnitude of estimated effective migration rates per generation among populations in the two taxa are below the threshold (2 Nm∼1; Table 3) that would impede populations from accumulating divergence by genetic drift (Wright 1931; Pinho & Hey 2010). This, together with the marked genetic structure of their respective contemporary populations (Fig. 1 and Supporting information S3-4), indicates that the two taxa show extraordinarily limited dispersal capacity in absolute terms. Overall, these results are in agreement with previous research documenting increased genetic differentiation accompanying evolutionary transitions to flightlessness (McCulloch et al. 2019) and in line with comparative landscape genetic (Ortego et al. 2015; Phillipsen et al. 2015) and macroecological (Riginos et al. 2014; Singhal et al. 2018) studies reporting increased genetic structure in taxa with more limited dispersal capacity (Waters et al. 2020). Our results support the notion that evolutionary transitions toward reduced dispersal capacity can

promote genetic divergence and be a key component of incipient stages of speciation (Ikeda et al. 2012; Waters et al. 2020), particularly among organisms distributed in topographically complex landscapes (Noguerales et al. 2016; González-Serna et al. 2019; McCulloch et al. 2019; Tonzo et al. 2019).

PAST DEMOGRAPHIC HISTORY

Demographic reconstructions indicate that populations from the two taxa experienced parallel demographic declines starting at the onset of the Holocene that have resulted in extraordinary reductions of their effective population sizes (>99%) since the end of the last glacial period (Fig. 3). The two taxa are nowadays primarily distributed in the montane, alpine, and subalpine thermoclimatic belts of the island, occupying similar xeric open habitats dominated by thorny and dwarf shrub formations (e.g., *Juniperus* sp., *Genista* sp., *Erica* sp., etc.; Braud et al. 2002; Boitier et al. 2006). However, an old record of *C. c. corsicus* at lower elevations (Col de Teghime, 530 m; Pfau 1984) suggests that their distributions might be more limited by the presence of adequate microhabitats than by elevation per se. The Holocene range expansion of Mediterranean and temperate forests, nowadays covering most natural areas of Corsica, are likely to have progressively pushed to higher elevations the open shrub formations occupied by the two taxa (Reille et al. 1997). This postglacial shrink of suitable habitats probably led to the confinement of populations in sky-islands, resulting in severe demographic declines after the end of the last glacial period and extreme genetic fragmentation of relictual contemporary populations of the two taxa (Fig. 1). On the contrary, demographic expansions during the coldest stages of the Pleistocene (Fig. 3) likely contributed to put the two taxa into geographical contact, which might have facilitated historical gene exchange. In this line, coalescent-based analyses support that postdivergence gene flow took place until the last glacial period (29-35 ka; Table 3), coinciding with the severe demographic declines experienced by the two taxa according to genomic-based reconstructions of changes in N_e through time (Fig. 3). Collectively, our results suggest strong fragmentation of populations in sky islands during interglacials and population reconnections and demographic expansions during cold glacial periods, which is congruent with the "interglacial refugia model" (*sensu* Bennett & Provan 2008; Stewart et al. 2010) documented in other alpine and montane organisms from temperate and tropical latitudes (e.g., Wang et al. 2013; He et al. 2016; Camacho-Sánchez et al. 2018). This contrasts with studies on other alpine organisms from temperate regions that were more extensively glaciated and for which genetic-based demographic inferences support isolation and divergence in glacial refugia and demographic expansions and admixture during interglacial periods (Carstens & Knowles 2007b; Schoville et al. 2011; Maier et al. 2019).

RECENT EVOLUTION OF REPRODUCTIVE ISOLATION?

A conclusive line of evidence supporting the taxonomic distinctiveness of *C. c. corsicus* and *C. c. pascuorum* is their assignment to distinct genetic clusters and apparent lack of contemporary gene flow in Col de Verde (i.e., "genotypic cluster species concept"; sensu Mallet 1995; DeQueiroz 2007), the only known locality where the two taxa co-occur (Pfau 1984; Massa 1994). We did not find first generation hybrids or backcrosses among genotyped individuals (Fig. 1 and Supporting information Fig. S3) or the presence of phenotypically intermediate individuals in this locality (Joaquín Ortego, pers. obs. 2019; Pfau 1984). Although our sample sizes are small and, thus, we cannot categorically discard that the two taxa sporadically interbreed, the fact that levels of genetic introgression are not disproportionately higher in this sympatric population (*D*-statistic tests; Supporting information Table S1) suggests that this phenomenon is infrequent or rarely transcends first-generation hybrids. Given that the presence of the two taxa in this locality was reported >35 years ago (Pfau 1984), their co-occurrence does not seem to be a consequence of a recent expansion event and, thus, they have had ample opportunity (>35 generations) to interbreed and experience genetic introgression. These lines of evidence suggest that reproductive isolation, developed through the progressive accumulation of barriers to gene flow via genetic drift (Coyne & Orr 1989; Sasa et al. 1998; Fitzpatrick 2002) or other mechanisms (Barton & Hewitt 1985; Butlin 1995; Barton 2001; Ortiz-Barrientos et al. 2004; Pfennig 2016), had probably already evolved when the two taxa became sympatric in Col de Verde. Although Pfau (1984) described the two taxa to be syntopic in this locality (i.e., the mixed co-occurrence of long- and short-winged forms), during our sampling we found that they inhabit the same thorny shrub formations of *Genista lobelii* but occupy habitat patches separated ca. 200 m apart (see Supporting information Fig. S9). This suggests that some sort of spatial segregation or subtle differences in microhabitat preferences might be at play, which could explain why the two species very rarely co-occur (Massa 1994). The fact that the two taxa occupy the same habitats (Braud et al. 2002; Boitier et al. 2006), present identical phenologies (Pfau 1984; Massa 1994), and show undistinguishable songs and courtship behaviors (Ragge & Reynolds 1998), leave pheromonal, tactile, or visual components of mate recognition (e.g., Ritchie 1990) or genital or gamete incompatibility (e.g., Tatarnic & Cassis 2013; Huang et al. 2020) as the only prezygotic reproductive barrier mechanisms that might explain the apparent lack of contemporary hybridization.

CONCLUSIONS

According to expectations from differences in dispersal capacity, our analyses support historical asymmetric gene flow from the long- to the short-winged taxon and lower or absent

contemporary effective migration rates and deeper divergences among populations of the flightless *C. c. corsicus*. Our genomic data also support reproductive isolation and the distinct taxonomic position of *C. c. corsicus* and *C. c. pascuorum*, which should be upgraded to their original full-species status (Chopard 1924): *Chorthippus* (*Glyptobothrus*) *corsicus* (Chopard 1924) and *Chorthippus* (*Glyptobothrus*) *pascuorum* (Chopard 1924) (for a list of synonyms, see Cigliano et al. 2020). These results point to a within-island diversification scenario, which has been rarely reported in short-horned grasshoppers but is not surprising given the relatively large size of the island of Corsica (>8000 km^2) and its extraordinarily complex topography (many peaks >2000 m.a.s.l.). Future hybridization attempts in the laboratory considering sympatric/allopatric populations of the species, detailed morphometric studies of genitalic structures, spatially explicit landscape genetic analyses, formal studies on ecological and microhabitat preferences, and monitoring of population persistence (i.e., local extinction rates) could contribute to shed further light on the processes underlying geographical and phenotypic diversification, reproductive isolation, and historical range dynamics in the two taxa. Likewise, the formal study of speciation rates in relation with wing size variation within the subgenus *Glyptobothrus* might help to elucidate the processes underlying the diversification of this speciose complex of grasshoppers and deepen into the understanding of the evolutionary consequences of dispersal reduction (Harvey et al. 2019).

AUTHOR CONTRIBUTIONS

JO conceived the study, collected the samples, analysed the data and wrote the manuscript. All authors designed the study, interpreted the data, and contributed to the writing and editing of the manuscript.

ACKNOWLEDGMENTS

We are grateful to Mamen Ramírez for preparing genomic libraries, Neda Moradin (The Centre for Applied Genomics) for Illumina sequencing, and three anonymous referees for their constructive and valuable comments on an earlier version of the manuscript. Logistical support was provided by Laboratorio de Ecología Molecular (LEM-EBD) from Estación Biológica de Doñana. We also thank to Centro de Supercomputación de Galicia (CESGA) and Doñana's Singular Scientific-Technical Infrastructure (ICTS-RBD) for access to computer resources. JGR and VN were supported by "Juan de la Cierva-Formación" fellowships (FJC2018-035899-I and FJC2018-035611-I, respectively) funded by the Spanish Ministry of Science and Innovation and the European Regional Development Fund (ERDF). This study was funded by the Spanish Ministry of Economy and Competitiveness and the European Regional Development Fund (ERDF) (CGL2014-54671-P, CGL2017-83433-P, and RYC-2013-12501).

CONFLICT OF INTEREST

The authors declare no conflict of interest.

[Corrections added on May 6, 2021 after first online publication: "DATA ARCHIVING" section was added.]

DATA ARCHIVING

Raw Illumina reads have been deposited at the NCBI Sequence Read Archive (SRA) under BioProject PRJNA702631. Alignments, SNP datasets, and input files for all analyses are archived and available on Dryad (https://doi.org/10.5061/dryad.bg79cnp9q).

LITERATURE CITED

Barton, N. H. 2001. The role of hybridization in evolution. Mol. Ecol. 10:551–568.

———. 2020. On the completion of speciation. Philos. Trans. R. Soc. Lond. B 375:20190530.

Barton, N. H., and G. M. Hewitt. 1985. Analysis of hybrid zones. Annu. Rev. Ecol. Evol. Syst. 16:113–148.

Bennett, K. D., and J. Provan. 2008. What do we mean by refugia? Quat. Sci. Rev. 27:2449–2455.

Boitier, E., D. Petit, and O. Bardet. 2006. Contribution a la connaissance des Orthopteroides de Corse (Orthoptera, Phasmoptera, Mantodea) [Contribution to the knowledge on the Orthopteroidea of Corsica (Orthoptera, Phasmoptera, Mantodea)]. Entomologiste (Paris) 62:129–145.

Bouckaert, R., J. Heled, D. Kuhnert, T. Vaughan, C. H. Wu, D. Xie, M. A. Suchard, A. Rambaut, and A. J. Drummond. 2014. BEAST2: A software platform for Bayesian evolutionary analysis. PLoS Comput. Biol. 10:e1003537.

Bouckaert, R. R. 2010. DENSITREE: Making sense of sets of phylogenetic trees. Bioinformatics 26:1372–1373.

Braud, Y., E. Sardet, and D. Morin. 2002. Actualisation du catalogue des orthopteroides de l'ile de Corse (France) [Update of the catalogue of Orthopteroidea of Corsica (France)]. Materiaux Entomocenotiques 7:5–22.

Bryant, D., R. Bouckaert, J. Felsenstein, N. A. Rosenberg, and A. RoyChoudhury. 2012. Inferring species trees directly from biallelic genetic markers: Bypassing gene trees in a full coalescent analysis. Mol. Biol. Evol. 29:1917–1932.

Burnham, K. P., and D. R. Anderson. 2002. Model selection and multimodel inference: A practical information-theoretic approach. Springer, New York.

Butlin, R. K. 1995. Reinforcement—An idea evolving. Trends Ecol. Evol. 10:432–434.

Camacho-Sánchez, M., I. Quintanilla, M. T. R. Hawkins, F. Y. Y. Tuh, K. Wells, J. E. Maldonado, and J. A. Leonard. 2018. Interglacial refugia on tropical mountains: Novel insights from the summit rat (*Rattus baluensis*), a Borneo mountain endemic. Divers. Distrib. 24:1252–1266.

Cárdenas, A. M., P. Gallardo, L. Moyano, and J. J. Presa. 2017. Autecology, feeding preferences and reproductive biology of *Chorthippus* (*Glyptobothrus*) *vagans* (Eversmann, 1848) (Orthoptera: Gomphocerinae) in Mediterranean ecosystems. Bull. Entomol. Res. 107:21–31.

Carstens, B. C., and L. L. Knowles. 2007a. Estimating species phylogeny from gene-tree probabilities despite incomplete lineage sorting: An example from *Melanoplus* grasshoppers. Syst. Biol. 56:400–411.

———. 2007b. Shifting distributions and speciation: species divergence during rapid climate change. Mol. Ecol. 16:619–627.

Catchen J., Hohenlohe Paul A., Bassham S., Amores A., Cresko William A. 2013. STACKS: an analysis tool set for population genomics. Molecular Ecology 22(11):3124–3140. https://doi.org/10.1111/mec.12354.

Chifman, J., and L. Kubatko. 2014. Quartet inference from SNP data under the coalescent model. Bioinformatics 30:3317–3324.

Chopard, L. 1924. Essai sur la fauna des Orthopteres de la Corse. Ann. Soc. Entomol. Fr. 92:253–286.

Cigliano, M. M., H. Braun, D. C. Eades, and D. Otte. 2020. Orthoptera species file. Version 5.0/5.0. Available at http://orthoptera.speciesfile.org/ (accessed February 3, 2021).

Coyne, J. A., and H. A. Orr. 1989. Patterns of speciation in *Drosophila*. Evolution 43:362–381.

Coyne, J. A., H. A. Orr. 2004. Speciation. Sinauer Associates, Sunderland.

Darwin, C. R. 1859. On the origin of the species by natural selection. John Murray, London.

De Queiroz, K. 2007. Species concepts and species delimitation. Syst. Biol. 56:879–886.

Defaut, B. 2014. Biometrie des types des Caeliferes de France (Orthoptera) 4. Mensurations chez les Acrididae Gomphocerinae. -5. Corrections et supplements [Biometrics of the type specimens of the Caelifera of France (Orthoptera) 4. Measurements of Acrididae Gomphocerinae. -5. Corrections and supplements]. Materiaux Orthopteriques et Entomocenotiques 19:5–56.

Dhuyvetter, H., F. Hendrickx, E. Gaublomme, and K. Desender. 2007. Differentiation between two salt marsh beetle ecotypes: Evidence for ongoing speciation. Evolution 61:184–193.

Durand, E. Y., N. Patterson, D. Reich, and M. Slatkin (2011). Testing for ancient admixture between closely related populations. Mol. Biol. Evol. 28:2239–2252.

Dussex, N., A. Chuah, and J. M. Waters. 2016. Genome-wide SNPs reveal fine-scale differentiation among wingless alpine stonefly populations and introgression between winged and wingless forms. Evolution 70:38–47.

Earl, D. A., and B. M. vonHoldt. 2012. STRUCTURE HARVESTER: A website and program for visualizing STRUCTURE output and implementing the Evanno method. Conserv. Genet. Resour. 4:359–361.

Eaton, D. A. R. 2014. PYRAD: Assembly of *de novo* RADseq loci for phylogenetic analyses. Bioinformatics 30:1844–1849.

Eaton, D. A. R., and R. H. Ree. 2013. Inferring phylogeny and introgression using RADseq data: An example from flowering plants (Pedicularis: Orobanchaceae). Syst. Biol. 62:689–706.

Evanno, G., S. Regnaut, and J. Goudet. 2005. Detecting the number of clusters of individuals using the software STRUCTURE: a simulation study. Mol. Ecol. 14:2611–2620.

Excoffier, L., G. Laval, and S. Schneider. 2005. ARLEQUIN ver. 3.0: An integrated software package for population genetics data analysis. Evol. Bioinform. Online 1:47–50.

Excoffier, L., I. Dupanloup, E. Huerta-Sánchez, V. C. Sousa, and M. Foll. 2013. Robust demographic inference from genomic and SNP data. PLoS Genet. 9:e1003905.

Feder, J. L., S. M. Flaxman, S. P. Egan, A. A. Comeault, and P. Nosil. 2013. Geographic mode of speciation and genomic divergence. Annu. Rev. Ecol. Evol. Syst. 44: 73–97.

Fitzpatrick, B. M. 2002. Molecular correlates of reproductive isolation. Evolution 56:191–198.

Flouri, T., X. Y. Jiao, B. Rannala, and Z. H. Yang. 2018. Species tree inference with BPP using genomic sequences and the multispecies coalescent. Mol. Biol. Evol. 35:2585–2593.

Fu, Y.-X. 1997. Statistical tests of neutrality of mutations against population growth, hitchhiking and backgroud selection. Genetics 147:915–925.

Gilbert, K. J., R. L. Andrew, D. G. Bock, M. T. Franklin, N. C. Kane, J. S. Moore, B. T. Moyers, S. Renaut, D. J. Rennison, T. Veen, and T. H. Vines. 2012. Recommendations for utilizing and reporting population genetic analyses: The reproducibility of genetic clustering using the program STRUCTURE. Mol. Ecol. 21:4925–4930.

González-Serna, M. J., P. J. Cordero, and J. Ortego. 2019. Spatiotemporally explicit demographic modelling supports a joint effect of historical barriers to dispersal and contemporary landscape composition on structuring genomic variation in a red-listed grasshopper. Mol. Ecol. 28:2155–2172.

Harrison, R. G. 1980. Dispersal polymorphisms in insects. Annu. Rev. Ecol. Evol. Syst. 11:95–118.

Harvey Michael G., Singhal S., and Rabosky Daniel L.. 2019. Beyond reproductive isolation: Demographic controls on the speciation process. Annual Review of Ecology, Evolution, and Systematics 50 (1): 75 –95. https://doi.org/10.1146/annurev-ecolsys-110218-024701.

Hendrickx, F., T. Backeljau, W. Dekoninck, S. M. Van Belleghem, V. Vandomme, and C. Vangestel. 2015. Persistent inter- and intraspecific gene exchange within a parallel radiation of caterpillar hunter beetles (*Calosoma* sp.) from the Galapagos. Mol. Ecol. 24:3107–3121.

He, K., N. Q. Hu, X. Chen, J. T. Li, and X. L. Jiang. 2016. Interglacial refugia preserved high genetic diversity of the Chinese mole shrew in the mountains of southwest China. Heredity 116:23–32.

Hey, J. 2006. Recent advances in assessing gene flow between diverging populations and species. Curr. Opin. Genet. Dev. 16:592–596.

Hochkirch, A., and M. Damerau. 2009. Rapid range expansion of a wing-dimorphic bush-cricket after the 2003 climatic anomaly. Biol. J. Linn. Soc. 97:118–127.

Huang, J. P., J. G. Hill, J. Ortego, and L. L. Knowles. 2020. Paraphyletic species no more: Genomic data resolve a Pleistocene radiation and validate morphological species of the *Melanoplus scudderi* complex (Insecta: Orthoptera). Syst. Entomol. 45:594–605.

Ikeda, H., M. Nishikawa, and T. Sota. 2012. Loss of flight promotes beetle diversification. Nat. Commun. 3:648.

Jacquemyn, H., R. Brys, O. Honnay, and I. Roldán-Ruiz. 2012. Asymmetric gene introgression in two closely related *Orchis* species: Evidence from morphometric and genetic analyses. BMC Evol. Biol. 12:178.

Jakobsson, M., and N. A. Rosenberg. 2007. CLUMPP: A cluster matching and permutation program for dealing with label switching and multimodality in analysis of population structure. Bioinformatics 23:1801–1806.

Janes, J. K., J. M. Miller, J. R. Dupuis, R. M. Malenfant, J. C. Gorrell, C. I. Cullingham, and R. L. Andrew. 2017. The $K = 2$ conundrum. Mol. Ecol. 26:3594–3602.

Jombart, T. 2008. Adegenet: A R package for the multivariate analysis of genetic markers. Bioinformatics 24:1403–1405.

Keightley, P. D., R. W. Ness, D. L. Halligan, and P. R. Haddrill. 2014. Estimation of the spontaneous mutation rate per nucleotide site in a *Drosophila melanogaster* full-sib family. Genetics 196:313–320.

Keightley, P. D., A. Pinharanda, R. W. Ness, F. Simpson, K. K. Dasmahapatra, J. Mallet, J. W. Davey, and C. D. Jiggins. 2015. Estimation of the spontaneous mutation rate in *Heliconius melpomene*. Mol. Biol. Evol. 32:239–243.

Kitson, J. J. N., B. H. Warren, C. Thebaud, D. Strasberg, and B. C. Emerson. 2018. Community assembly and diversification in a species-rich radiation of island weevils (Coleoptera: Cratopini). J. Biogeogr. 45:2016–2026.

Kuhlemann, J., W. Frisch, B. Székely, I. Dunkl, M. Danišík, and I. Krumrei. 2005. Würmian maximum glaciation in Corsica. Aust. J. Earth Sci. 97:68–81.

Laiolo, P., J. C. Illera, and J. R. Obeso. 2013. Local climate determines intra- and interspecific variation in sexual size dimorphism in mountain grasshopper communities. J. Evol. Biol. 26:2171–2183.

Leaché, A. D., R. B. Harris, B. Rannala, and Z. H. Yang. 2014. The influence of gene flow on species tree estimation: A simulation study. Syst. Biol. 63:17–30.

Liu, X. M. and Y. X. Fu. 2015. Exploring population size changes using SNP frequency spectra. Nat. Genet. 47:555–559.

Maier, P. A., A. G. Vandergast, S. M. Ostoja, A. Aguilar, and A. J. Bohonak. 2019. Pleistocene glacial cycles drove lineage diversification and fusion in the Yosemite toad (*Anaxyrus canorus*). Evolution 73:2476–2496.

Mallet, J. 1995. A species definition for the modern synthesis. Trends Ecol. Evol. 10:294–299.

Massa, B. 1994. Su alcuni ortotteri poco noti delle isole Mediterranee (Insecta: Orthoptera). Nat. Sicil. 18:239–253.

McCulloch, G. A., B. J. Foster, L. Dutoit, T. Ingram, E. Hay, A. J. Veale, P. K. Dearden, and J. M. Waters. 2019. Ecological gradients drive insect wing loss and speciation: The role of the alpine treeline. Mol. Ecol. 28:3141–3150.

McCulloch, G. A., G. P. Wallis, and J. M. Waters. 2009. Do insects lose flight before they lose their wings? Population genetic structure in subalpine stoneflies. Mol. Ecol. 18:4073–4087.

Morales, A. E., N. D. Jackson, T. A. Dewey, B. C. O'Meara, and B. C. Carstens. 2017. Speciation with gene flow in North American *Myotis* bats. Syst. Biol. 66:440–452.

Noguerales, V., P. J. Cordero, and J. Ortego. 2016. Hierarchical genetic structure shaped by topography in a narrow-endemic montane grasshopper. BMC Evol. Biol. 16:96.

Nosil, P. 2008. Speciation with gene flow could be common. Mol. Ecol. 17:2103–2106.

Ortego, J., V. García-Navas, V. Noguerales, and P. J. Cordero. 2015. Discordant patterns of genetic and phenotypic differentiation in five grasshopper species codistributed across a microreserve network. Mol. Ecol. 24:5796–5812.

Ortiz-Barrientos, D., B. A. Counterman, and M. A. F. Noor. 2004. The genetics of speciation by reinforcement. PLoS Biol. 2:2256–2263.

Peterson, B. K., J. N. Weber, E. H. Kay, H. S. Fisher, and H. E. Hoekstra. 2012. Double digest RADseq: An inexpensive method for *de novo* SNP discovery and genotyping in model and non-model species. PLoS One 7:e37135.

Pfau, H. K. 1984. Verbreitung und Gesänge kleiner korsischer *Omocestus*- (bzw. *Chorthippus*-) Arten [Distribution and song patterns of dwad Corsican species of *Omocestus* (*Chorthippus* respectively)]. Verh. Dtsch. Zool. Ges. 77:267.

Pfennig, K. S. 2016. Reinforcement as an initiator of population divergence and speciation. Curr. Zool. 62:145–154.

Phillipsen, I. C., E. H. Kirk, M. T. Bogan, M. C. Mims, J. D. Olden, and D. A. Lytle. 2015. Dispersal ability and habitat requirements determine landscape-level genetic patterns in desert aquatic insects. Mol. Ecol. 24:54–69.

Pickrell, J. K., and J. K. Pritchard. 2012. Inference of population splits and mixtures from genome-wide allele frequency data. PLoS Genet. 8:e1002967.

Pinho, C., and J. Hey. 2010. Divergence with gene flow: Models and data. Annu. Rev. Ecol. Evol. Syst. 41:215–230.

Pritchard, J. K., M. Stephens, and P. Donnelly. 2000. Inference of population structure using multilocus genotype data. Genetics 155:945–959.

R Core Team. 2020. R: A language and environment for statistical computing. R Foundation for Statistical Computing, Vienna, Austria. Available at https://www.R-project.org/ (accessed February 3, 2021).

Ragge, D. R., and W. J. Reynolds. 1998. The songs of the grasshoppers and crickets of western Europe. Harley Books, Colchester.

Reille, M., J. Gamisans, J. L. deBeaulieu, and V. Andrieu. 1997. The lateglacial at Lac de Creno (Corsica, France): A key site in the western Mediterranean Basin. New Phytol. 135:547–559.

Riginos, C., Y. M. Buckley, S. P. Blomberg, and E. A. Treml. 2014. Dispersal capacity predicts both population genetic structure and species richness in reef fishes. Am. Nat. 184:52–64.

Ritchie, M. G. 1990. Are differences in song responsible for assortafive mating between subspecies of the grasshopper *Chorthippus parallelus* (Orthoptera: Acrididae)? Anim. Behav. 39:685–691.

Roff, D. A. 1990. The evolution of flightlessness in insects. Ecol. Monogr. 60:389–421.

———. 1994. Habitat persistence and the evolution of wing dimorphism in insects. Am. Nat. 144:772–798.

Rosenberg, N. A. 2004. Distruct: A program for the graphical display of population structure. Mol. Ecol. Notes 4:137–138.

Roux C., Fraïsse C., Romiguier J., Anciaux Y., Galtier N., and Bierne N. 2016. Shedding light on the grey zone of speciation along a continuum of genomic divergence. PLOS Biology 14(12):e2000234. https://doi.org/10.1371/journal.pbio.2000234.

Rozas, J., A. Ferrer-Mata, J. C. Sánchez-DelBarrio, S. Guirao-Rico, P. Librado, S. E. Ramos-Onsins, and A. Sánchez-Gracia. 2017. DNASP 6: DNA sequence polymorphism analysis of large data sets. Mol. Biol. Evol. 34:3299–3302.

Sasa, M. M., P. T. Chippindale, and N. A. Johnson. 1998. Patterns of postzygotic isolation in frogs. Evolution 52:1811–1820.

Scattolini, M. C., V. Confalonieri, A. Lira-Noriega, S. Pietrokovsky, and M. M. Cigliano. 2018. Diversification mechanisms in the Andean grasshopper genus *Orotettix* (Orthoptera: Acrididae): Ecological niches and evolutionary history. Biol. J. Linn. Soc. 123:697–711.

Schoville, S. D., M. Stuckey, and G. K. Roderick. 2011. Pleistocene origin and population history of a neoendemic alpine butterfly. Mol. Ecol. 20:1233–1247.

Simmons, A. D., and C. D. Thomas. 2004. Changes in dispersal during species' range expansions. Am. Nat. 164:378–395.

Singhal, S., H. T. Huang, M. R. Grundler, M. R. Marchan-Rivadeneira, I. Holmes, P. O. Title, S. C. Donnellan, and D. L. Rabosky. 2018. Does population structure predict the rate of speciation? A comparative test across Australia's most diverse vertebrate radiation. Am. Nat. 192:432–447.

Stewart, J. R., A. M. Lister, I. Barnes, and L. Dalen. 2010. Refugia revisited: Individualistic responses of species in space and time. Proc. R. Soc. Lond. B 277:661–671.

Swofford, D. L. 2002. PAUP*. Phylogenetic analysis using parsimony (*and other methods). Version 4. Sinauer Associates, Sunderland, MA.

Tajima, F. 1989. Statistical method for testing the neutral mutation hypothesis by DNA polymorphism. Genetics 123:585–595.

Tatarnic, N. J., and G. Cassis. 2013. Surviving in sympatry: Paragenital divergence and sexual mimicry between a pair of traumatically inseminating plant bugs. Am. Nat. 182:542–551.

Thome, M. T. C., and B. C. Carstens. 2016. Phylogeographic model selection leads to insight into the evolutionary history of four-eyed frogs. Proc. Natl. Acad. Sci. U.S.A. 113:8010–8017.

Tonzo, V., A. Papadopoulou, and J. Ortego. 2019. Genomic data reveal deep genetic structure but no support for current taxonomic designation in a grasshopper species complex. Mol. Ecol. 28:3869–3886.

———. 2020. Genomic footprints of an old affair: Single nucleotide polymorphism data reveal historical hybridization and the subsequent evolution of reproductive barriers in two recently diverged grasshoppers with partly overlapping distributions. Mol. Ecol. 29:2254–2268.

Van Belleghem, S. M., C. Vangestel, K. De Wolf, Z. De Corte, M. Most, P. Rastas, L. De Meester, and F. Hendrickx. 2018. Evolution at two time frames: Polymorphisms from an ancient singular divergence event fuel contemporary parallel evolution. PLoS Genet. 14:e1007796.

Veale, A. J., B. J. Foster, P. K. Dearden, and J. M. Waters. 2018. Genotyping-by-sequencing supports a genetic basis for wing reduction in an alpine New Zealand stonefly. Sci. Rep. 8:16275.

Vogler, A. P., and M. Timmermans. 2012. Speciation: Don't fly and diversify? Curr. Biol. 22:R284–R286.

Voisin, J.-F. 2003. Atlas des Orthoptères et des Mantides de France [Atlas of the grasshoppers and mantids of France]. Museum National d'Histoire Naturelle, Paris.

Wagner, D. L., and J. K. Liebherr. 1992. Flightlessness in insects. Trends Ecol. Evol. 7:216–220.

Walsh, B. 2001. Estimating the time to the most recent common ancestor for the Y chromosome or mitochondrial DNA for a pair of individuals. Genetics 158:897–912.

Wang, W. J., B. D. McKay, C. Y. Dai, N. Zhao, R. Y. Zhang, Y. H. Qu, G. Song, S. H. Li, W. Liang, X. J. Yang, E. Pasquet, and F. M. Lei. 2013. Glacial expansion and diversification of an East Asian montane bird, the green-backed tit (*Parus monticolus*). J. Biogeogr. 40:1156–1169.

Waters, J. M., B. C. Emerson, P. Arribas, and G. A. McCulloch. 2020. Dispersal reduction: Causes, genomic mechanisms, and evolutionary consequences. Trends Ecol. Evol. 35:512–522.

Whiting, M. F., S. Bradler, and T. Maxwell. 2003. Loss and recovery of wings in stick insects. Nature 421:264–267.

Wright, S. 1931. Evolution in Mendelian populations. Genetics 16:97–159.

Yang, M., Z. W. He, S. H. Shi, and C. I. Wu. 2017. Can genomic data alone tell us whether speciation happened with gene flow? Mol. Ecol. 26:2845–2849.

Yue, Q. Y., K. L. Wu, D. Y. Qiu, J. Hu, D. X. Liu, X. Y. Wei, J. Chen, and C. E. Cook. 2014. A formal re-description of the cockroach *Hebardina concinna* anchored on DNA barcodes confirms wing polymorphism and identifies morphological characters for field identification. PLoS One 9:e106789.

Zeng, Y., C. O'Malley, S. Singhal, F. Rahim, S. Park, X. Chen, and R. Dudley. 2020. A tale of winglets: Evolution of flight morphology in stick insects. Front. Ecol. Evol. 8:121.

Zera, A. J., and R. F. Denno. 1997. Physiology and ecology of dispersal polymorphism in insects. Annu. Rev. Entomol. 42:207–230.

Associate Editor: D. Filatov
Handling Editor: A. G. McAdam

Supporting Information

Additional supporting information may be found online in the Supporting Information section at the end of the article.

Table S1. Analyses of introgression using four-taxon *D*-statistic tests.
Table S2. Comparison of alternative population graph models tested using TREEMIX.
Table S3. Parameters inferred with FASTSIMCOAL2 under the model of speciation in strict isolation.
Figure S1. Number of reads per individual before and after different quality filtering steps.
Figure S2. Log probability of the data and the magnitude of ΔK for Bayesian clustering analyses in STRUCTURE.
Figure S3. Genetic assignment of individuals based on the results of Bayesian clustering analyses in STRUCTURE.
Figure S4. Principal component analyses (PCAs) of genetic variation.
Figure S5. Phylogenetic tree inferred with SVDQUARTETS.
Figure S6. Maximum-likelihood tree inferred with TREEMIX.
Figure S7. Phylogenetic tree and estimated divergence times using BPP.
Figure S8. Demographic history of the studied populations inferred using STAIRWAY PLOT.
Figure S9. Geographical location of the only known locality where the two taxa co-occur.